Supporting Information

Fluorine induced enhancement of surface polarization and crystallization of g-C$_3$N$_4$ for efficient charge separation

Xiaojuan Bai,*[a,b], Xuyu Wang [a], Xiongwei Lu [a], Boxuan Sun [a], Cong Wang [a], Tianqi Jia [a], Shanshan Hou [a], Ruilong Zong [c]

[a]*Key Laboratory of Urban Stormwater System and Water Environment (Beijing University of Civil Engineering and Architecture), Ministry of Education, Beijing 100044, China*

[b]*Beijing Engineering Research Center of Sustainable Urban Sewage System Construction and Risk Control, Beijing University of Civil Engineering and Architecture, Beijing 100044, China*

[c]*Department of Chemistry, Tsinghua University, Beijing 100084, China*

E-mail: *baixiaojuan@bucea.edu.cn   heixia.1986@163.com*

Section S1. Synthesis of bulk g-C$_3$N$_4$

A certain amount of urea powder was heated in an alumina crucible with a cover at 550 ℃ for 3 h with a heating rate of 10 ℃ min^{-1}. The resultant yellow powder was named bulk g-C$_3$N$_4$.

Section S2. Synthesis of F-doped g-C$_3$N$_4$ and g-C$_3$N$_4$-H$_2$O

F-doped g-C$_3$N$_4$ was synthesized as follows: 1 g of bulk g-C$_3$N$_4$ was dispersed in 15 mL HF ([HF] = 2 mol L^{-1}, 1 mol L^{-1}, 0.5 mol L^{-1}, 0.2 mol L^{-1}, and 0.1 mol L^{-1}) for 30 min. Then treating it in microwave digestion apparatus at 150 ℃ for 20 minutes at a heating rate of 30 ℃ min^{-1}. The resulting powder was washed with deionized water and absolute ethanol three times, followed by vacuum drying at 75 ℃ for 10 h. Besides, the g-C$_3$N$_4$-H$_2$O sample was synthesized by microwave etching with pure H$_2$O as the medium with the same experimental conditions for comparison.

Section S3. Photocatalytic degradation experiments and radical trapping experiments

The photocatalytic degradation of phenol ([phOH] = 5 ppm), bisphenol A ([BPA] = 5 ppm), diclofenac sodium ([DCF] = 5 ppm) and methylene blue ([MB] = 2×10^{-5} mol L^{-1}) solution were respectively conducted at room temperature in a visible light multi-position photochemical reactor in single-solute. In detail [1], 25 mg of sample powder was dispersed in 50 mL pollutants and ultrasonicated for 30 minutes to form a homogeneous composite solution. Then stir in dark for 30 minutes to reach adsorption equilibrium. Subsequently, the lamp was turned on to start the photocatalysis reaction and the process of degradation was reacted under simulated solar irradiation. For the detection of degradation products of phOH, BPA and DCF, 2 ml of the supernatant were removed every 1.5 h (t$_{total}$ = 7.5 h) and centrifuged (with the 0.45 μm PTFE filter) to remove the photocatalyst for determining the concentration of residual pollutants by HPLC (LC-20AT, Japan) with a tunable UV absorption detector at 270, 270 and 275 nm and a Roc-C18 column (150 mm×4.6 mm, 5 μm). And for MB solution, 2 ml of the supernatant were removed every 0.5 h (t$_{total}$ = 3 h) and the concentration of supernatant after filtering was continuously measured by using an ultraviolet-visible spectrophotometer (λ_{max} = 663 nm).
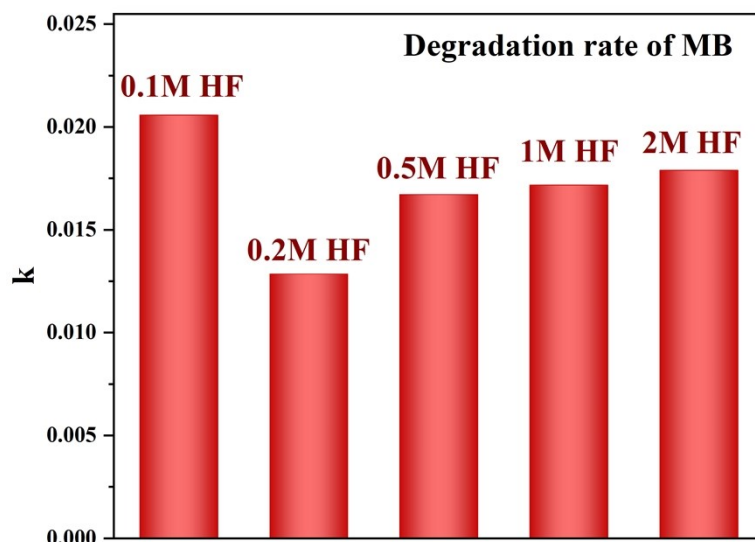
The degradation of MB solution at different wavelengths was carried out at room temperature in a multi-channel photocatalytic reaction system (PCX-50C Discover, PerfectLight). Specifically, 25 mg of catalyst was dispersed in 6 quartz tubes containing 50 ml MB solution

([MB] = $2×10^{-5}$ mol L^{-1}). Ultrasonicating for 30 minutes to form a homogeneous composite solution and putting them into the multichannel photocatalytic reaction system. Then the lamp was turned on to start the photocatalysis reaction. Finally, 2 ml of the supernatant were removed every 0.5 h (t_{total} = 3 h) and the concentration of supernatant after filtering was continuously measured by using an ultraviolet-visible spectrophotometer (λ_{max} = 663 nm).

Besides, we conducted phOH for the radical trapping experiments under xenon lamp irradiation. The scavenger for each reactive species was added to the reaction solution like that described for the photocatalytic experiment (above). The concentrations of tert-Butyl Alcohol (*t*BuOH), p-benzoquinone (PBQ) and EDTA-2Na as scavengers are $5×10^{-4}$ mol L^{-1}. The pseudo-first-order rate constant for contaminant photocatalytic degradation was obtained by performing a linear regression of the natural log of contaminant concentrations vs time.

[1] X.J. Bai, X.Y. Wang, X.W. Lu, Y.J. Liang, J.Q. Li, L.Y. Wu, H.Y. Li, Q. Hao, B.-J. Ni, C.C. Wang, Surface defective g-C$_3$N$_{4-x}$Cl$_x$ with unique spongy structure by polarization effect for enhanced photocatalytic removal of organic pollutants, J. Hazard. Mater., 398 (2020) 122897.

Section S4. The theoretical calculation

The electronic properties were analyzed for the structures of the bulk g-C$_3$N$_4$ and F-doped g-C$_3$N$_4$ using DFT calculation. A simplified DFT calculation was preceded on the CASTEP program. The generalized gradient approximation with the Perdew-Wang exchange-correlation functional (GG A-PW91) was employed for the exchange-correlation energy. Considering the weak van der Waals (vdW) interaction between interlayer included by the lamellar structure of g-C$_3$N$_4$, the OBS scheme which put forward by Ortmann, Bechstedt, and Schmidt and TS method which put forward by Tkatchenko and Scheffler [2]. The cutoff energy is 470 eV. Geometry relaxations are performed until the residual forces on each atom converged to be smaller than 0.05 eV Å^{-1}. This set of parameters guarantees that energy tolerance is within $2.0×10^{-5}$ eV per atom.

[2] F. Ortmann, F. Bechstedt, W.G. Schrnidt, Semiempiricalvan der Waals correction to the density functional description of solids and molecular structures, Phys. Rcv. B, 73 (2006) 205101.

Fig. S1 The degradation rate of MB solution by F-doped g-C_3N_4 etched by different concentrations of HF.
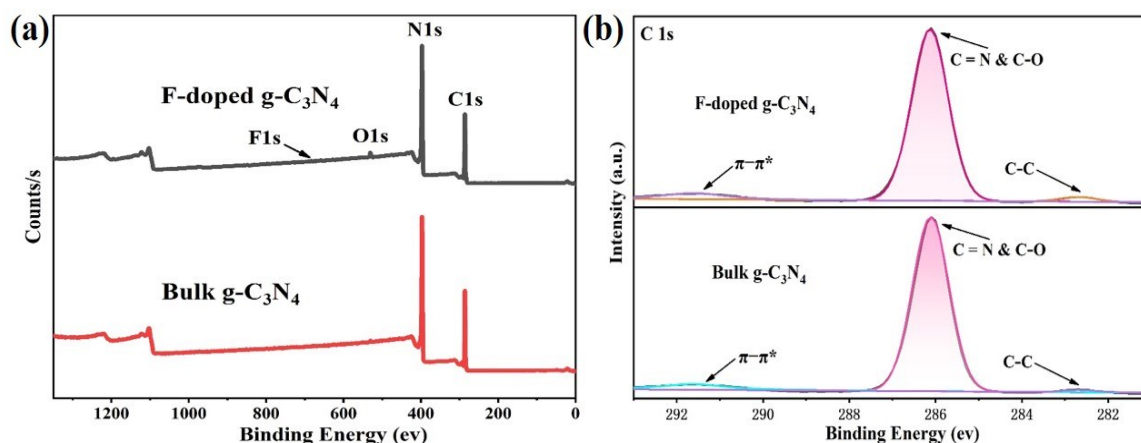
Fig. S2 (a) XPS survey spectra for F-doped g-C_3N_4 (C 1s, N 1s, O 1s, F 1s), g-C_3N_4-H_2O (C 1s, N 1s, O 1s) and bulk g-C_3N_4 (C 1s, N 1s, O 1s). (b) XPS C 1s spectrum of F-doped g-C_3N_4 and bulk g-C_3N_4.
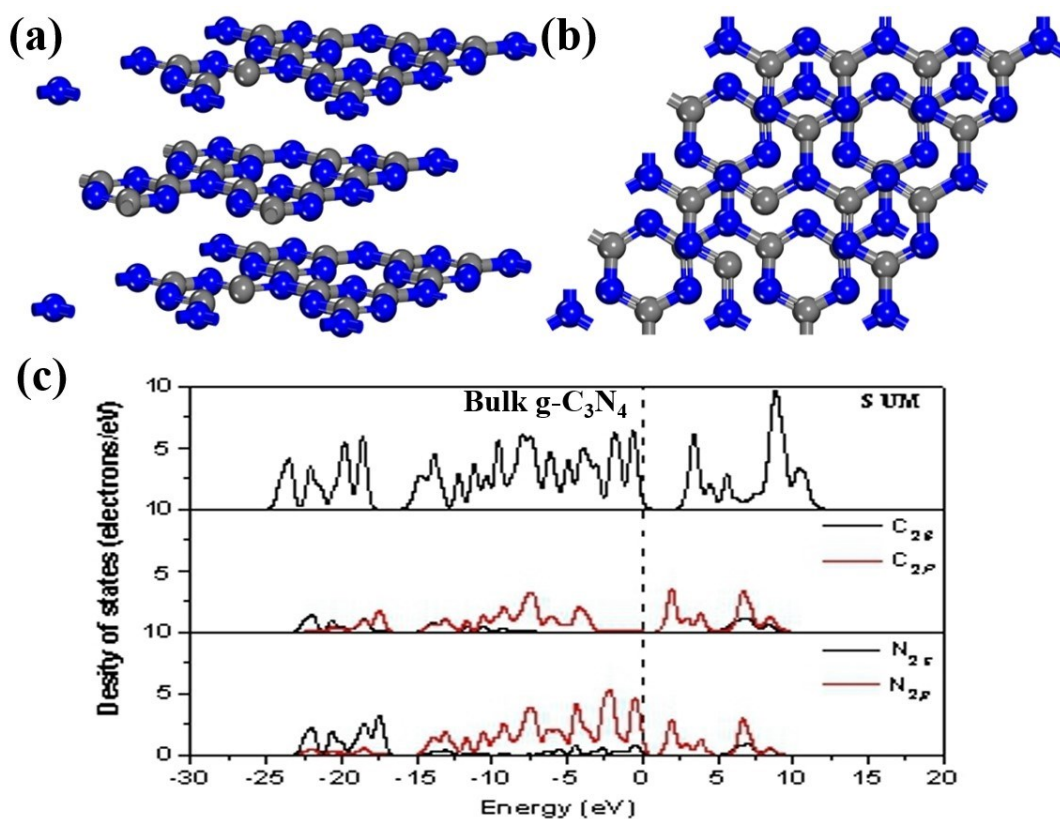
Fig. S3 (a) Front view and (b) Top view of bulk g-C$_3$N$_4$, where C, N, and F indicated as gray, dark blue and light blue spheres, respectively. (c) The first-principles calculations of energy (DOS) of bulk g-C$_3$N$_4$.

Section S5 An explanation for Wigner Seitz radius (RWIGS).

There are two major reasons involving the size of Wigner Seitz radius (RWIGS) and the orthonormalization of the atomic orbital. On one hand, the smaller size of RWIGS results in the smaller sum of the volume of the spheres around each atom compared to the volume of the system. The calculated total DOS is limited by the smaller RWIGS value. On the other hand, the atomic orbitals for different elements are not orthonormal [3], thus, the sum of the pDOS cannot be equal to the total DOS. Overall, the sum of the PDOS is always unequal to the total DOS considering the above-mentioned two reasons.

[3] M. Stefan, V.L. Deringer, A.L. Tchougréeff, R. Dronskowski, Analytic projection from plane-wave and PAW wavefunctions and application to chemical-bonding analysis in solids, J. comput. chem., 34 (2013) 2557-2567.
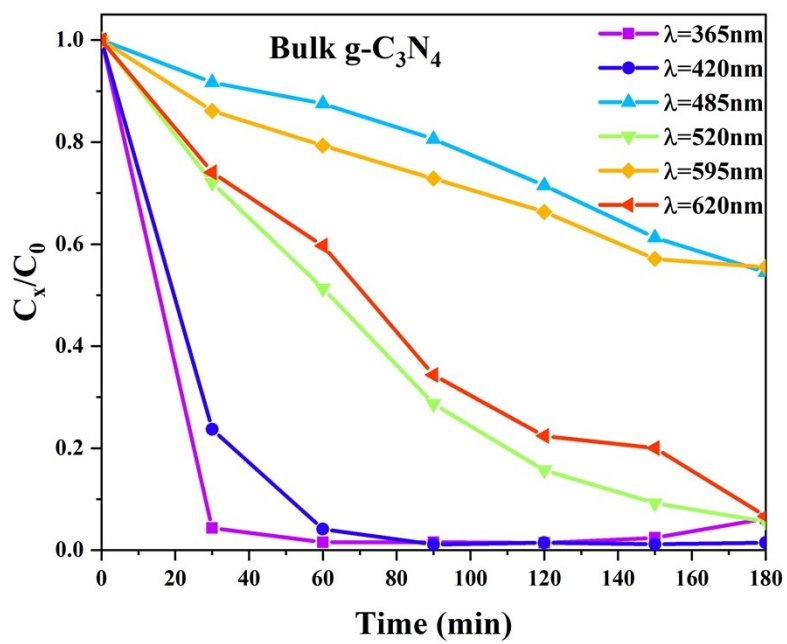
Fig. S4 The photodegradation efficiency of MB solution by using bulk g-C$_3$N$_4$ with different wavelengths of light.
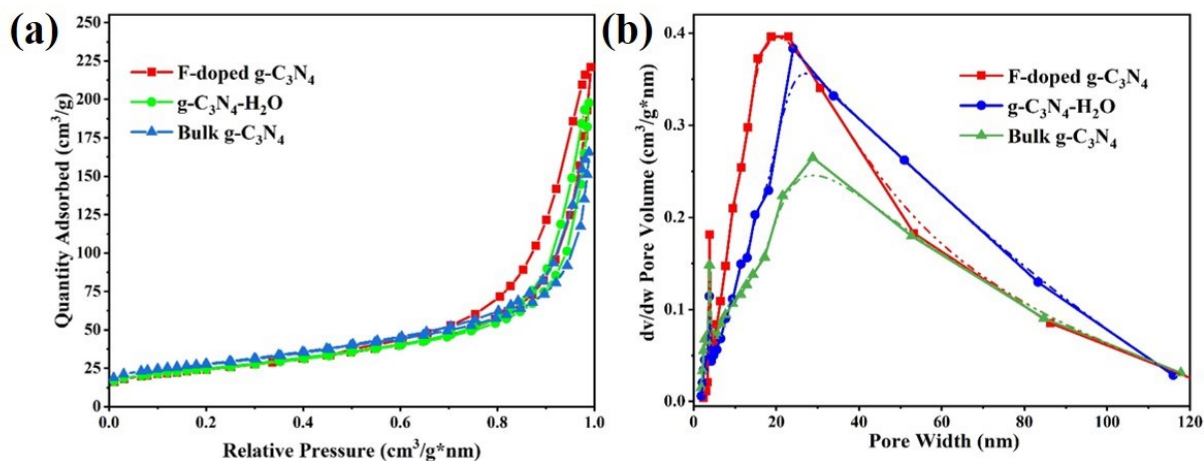
Fig. S5 (a) Nitrogen adsorption isotherms and (b) Barrett-Joyner-Halenda (BJH) adsorption pore-size distribution of F-doped g-C$_3$N$_4$, g-C$_3$N$_4$-H$_2$O, and bulk g-C$_3$N$_4$.

The specific surface areas and pore size distributions of three samples are analyzed by N$_2$ adsorption-desorption experiments. According to the IUPAC classification [4], the adsorption-desorption isotherms of all the samples revealed a type IV isotherm with an H4 hysteresis loop in the relative pressure range of 0.72-0.99, indicating the presence of mesopores [5].

[4] M. Thommes, K. Kaneko, A.V. Neimark, J.P. Olivier, F. Rodriguez-Reinoso, J. Rouquerol, K.S.W. Sing, Physisorption of gases, with special reference to the evaluation of surface area and pore size distribution (IUPAC Technical Report), Pure Appl. Chem., 87 (2015) 1051-1069.

[5] H. Katsumata, F. Higashi, Y. Kobayashi, I. Tateishi, M. Furukawa, S. Kaneco, Dual-defect-modified graphitic carbon nitride with boosted photocatalytic activity under visible light, Sci. Rep., 9 (2019) 14873.
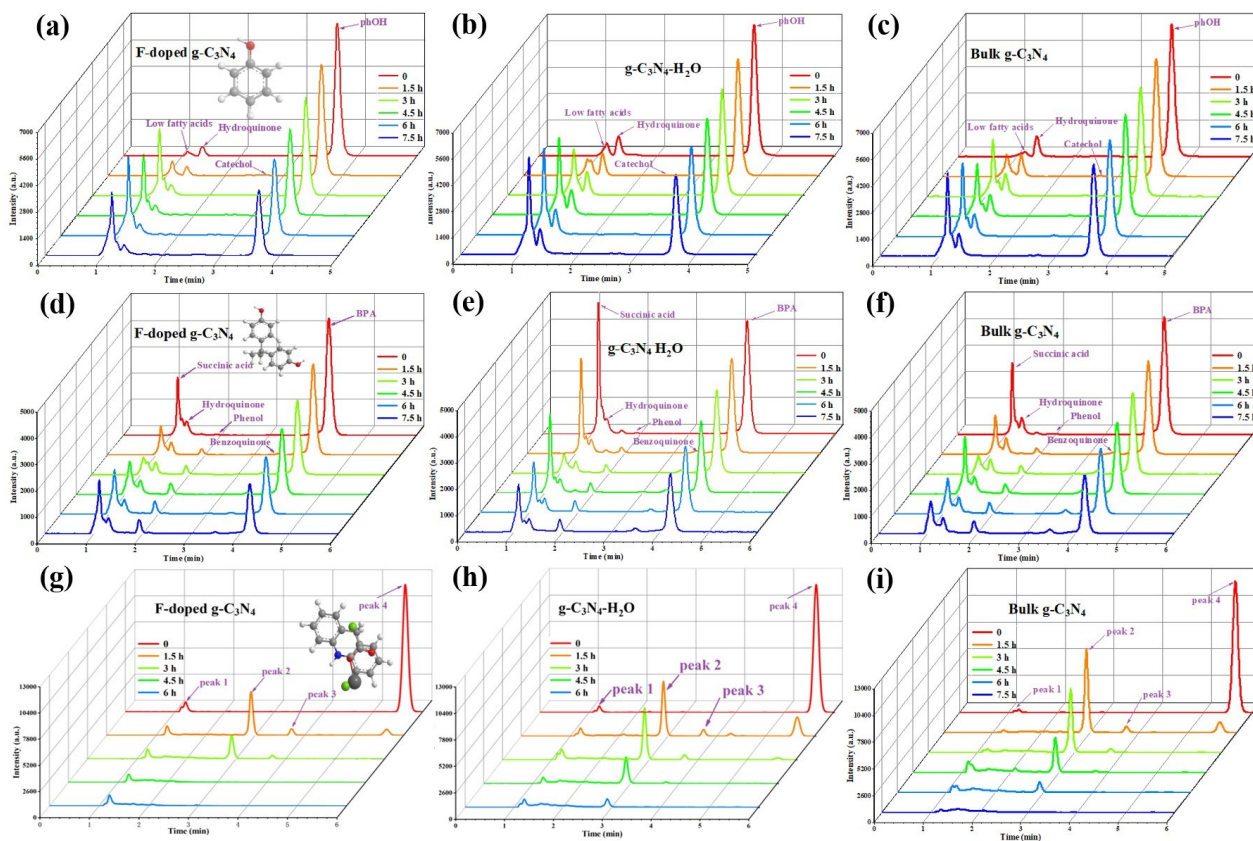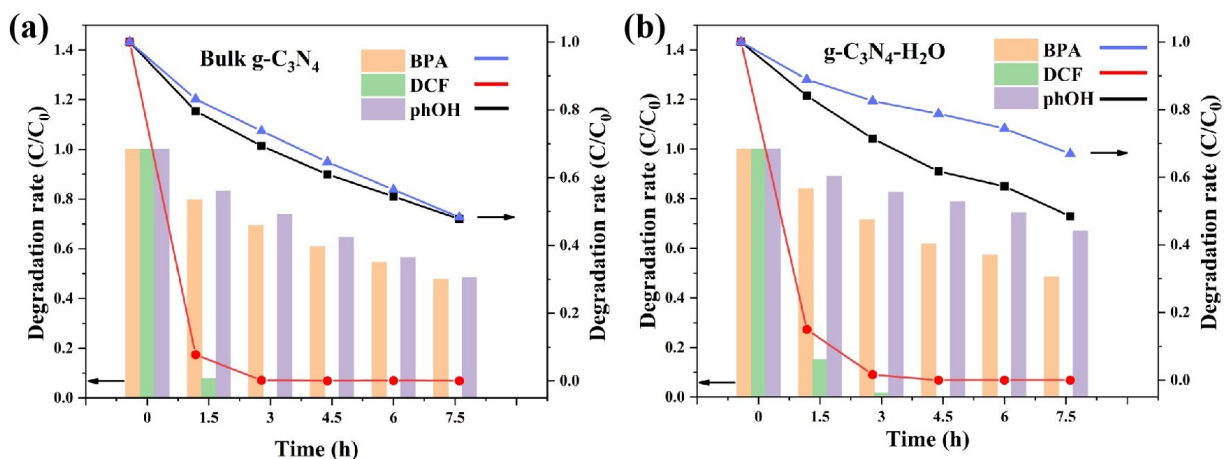
Fig. S6 HPLC diagram of (a-c) phOH, (d-f) BPA, and (g-i) DCF by three samples: (a, d, and g) F-doped g-C_3N_4, (b, e, and h) g-C_3N_4-H_2O, (c, f, and i) bulk g-C_3N_4.
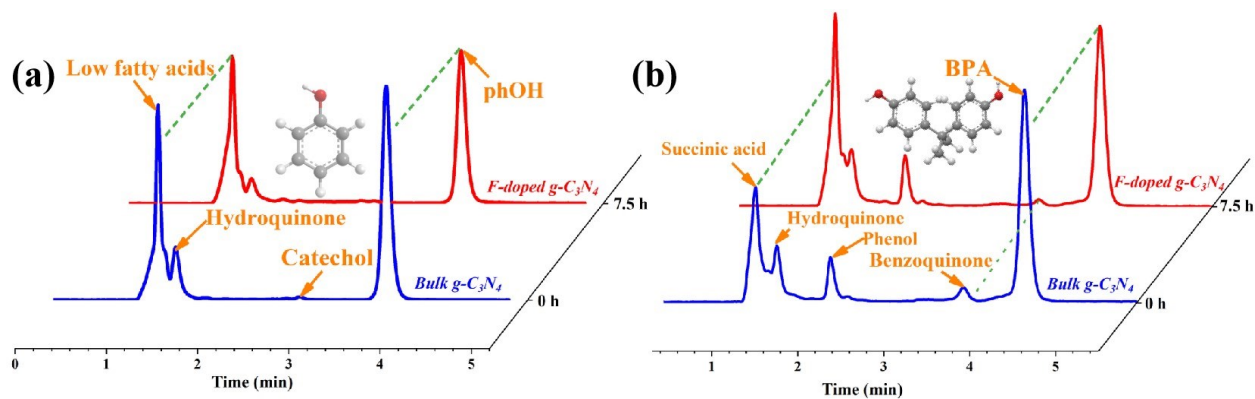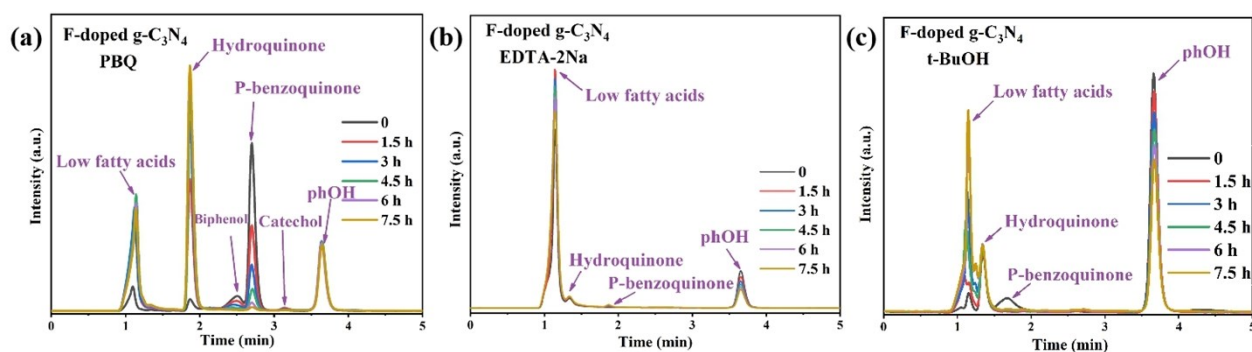

Fig. S7 HPLC diagram of (a) phOH and (b) BPA by F-doped g-C_3N_4 and bulk g-C_3N_4 at 0 hours and 7.5 hour.

8

Fig. S8 The degradation rates of (a) bulk g-C$_3$N$_4$ and (b) g-C$_3$N$_4$-H$_2$O for phOH, BPA and DCF. (The histogram corresponds to the left ordinate, and the broken line corresponds to the right ordinate.)

Fig. S9 (a) HPLC diagram of F-doped g-C$_3$N$_4$ degrading phOH with (b) p-benzoquinone (PBQ), (c) EDTA-2Na and (d) tert-butanol (tBuOH) as trapping scavengers.